

RESEARCH ARTICLE

Differential STAT gene expressions of *Penaeus monodon* and *Macrobrachium rosenbergii* in response to white spot syndrome virus (WSSV) and bacterial infections: Additional insight into genetic variations and transcriptomic highlights

Tze Chiew Christie Soo¹, Subha Bhassu^{1,2*}

1 Faculty of Science, Animal Genetics and Genome Evolutionary Laboratory (AGAGEL), Department of Genetics and Molecular Biology, Institute of Biological Sciences, University of Malaya, Kuala Lumpur, Malaysia, **2** Terra Aqua Laboratory, Centre for Research in Biotechnology for Agriculture (CEBAR), Research Management and Innovation Complex, University of Malaya, Kuala Lumpur, Malaysia

* subhabhassu@um.edu.my



OPEN ACCESS

Citation: Soo TCC, Bhassu S (2021) Differential STAT gene expressions of *Penaeus monodon* and *Macrobrachium rosenbergii* in response to white spot syndrome virus (WSSV) and bacterial infections: Additional insight into genetic variations and transcriptomic highlights. PLoS ONE 16(10): e0258655. <https://doi.org/10.1371/journal.pone.0258655>

Editor: Hoh Boon-Peng, UCSI University, MALAYSIA

Received: June 17, 2021

Accepted: October 4, 2021

Published: October 15, 2021

Copyright: © 2021 Soo, Bhassu. This is an open access article distributed under the terms of the [Creative Commons Attribution License](https://creativecommons.org/licenses/by/4.0/), which permits unrestricted use, distribution, and reproduction in any medium, provided the original author and source are credited.

Data Availability Statement: The study's minimal data set or raw data for the qPCR results were provided in the [Supporting information](#) document ([S1 Data](#)).

Funding: SB Institute of Pengurusan dan Penyelidikan (IPPP) RU 004G-2020 No, the funders did not play any role in all the above which is in the study design, data collection and analysis,

Abstract

Diseases have remained the major issue for shrimp aquaculture industry for decades by which different shrimp species demonstrated alternative disease resistance or tolerance. However, there had been insufficient studies on the underlying host mechanisms of such phenomenon. Hence, in this study, the main objective involves gaining a deeper understanding into the functional importance of shrimp STAT gene from the aspects of expression, sequence, structure, and associated genes. STAT gene was selected primarily because of its vital signalling roles in stress, endocrine, and immune response. The differential gene expressions of *Macrobrachium rosenbergii* STAT (*MrST*) and *Penaeus monodon* STAT (*PmST*) under White Spot Syndrome Virus (WSSV) and *Vibrio parahaemolyticus* *Vp*_{AHPND} infections were identified through qPCR analysis. Notably, during both pathogenic infections, *MrST* demonstrated significant gene expression down-regulations (during either early or later post-infection time points) whereas *PmST* showed only significant gene expression up-regulations. Important sequence conservation or divergence was highlighted through STAT sequence comparison especially amino acid alterations at 614 aa [K (Lysine) to E (Glutamic Acid)] and 629 aa [F (Phenylalanine) to V (Valine)] from *PmST* (AY327491.1) to *PmST* (disease tolerant strain). There were significant differences observed between in silico characterized structures of *MrST* and *PmST* proteins. Important functional differentially expressed genes (DEGs) in the aspects of stress, endocrine, immune, signalling, and structural were uncovered through comparative transcriptomic analysis. The DEGs associated with STAT functioning were identified including inositol 1,4,5-trisphosphate receptor, hsp90, caspase, ATP binding cassette transmembrane transporter, C-type Lectin, HMGB, ALF1, ALF3, superoxide dismutase, glutathione peroxidase, catalase, and TBK1. The main findings of this study are STAT differential gene expression patterns, sequence divergence,

decision to publish, or preparation of the manuscript. URL: www.cebar.um.edu.my.

Competing interests: The authors have declared that no competing interests exist.

structural differences, and associated functional DEGs. These findings can be further utilized for shrimp health or host response diagnostic studies. STAT gene can also be proposed as a suitable candidate for future studies of shrimp innate immune enhancement.

1.0 Introduction

The shrimp aquaculture industry is an important global economic sector especially for some middle- or low-level economies [1]. Vital shrimp species including *Litopenaeus vannamei*, *Penaeus monodon*, and *Macrobrachium rosenbergii* had majorly contributed to the annual global shrimp aquaculture production of roughly 6.0 million tonnes in year 2018 [2]. However, the shrimp aquaculture production had always been significantly impeded by various shrimp diseases which remained the top concern for aquaculture farmers [3]. These shrimp diseases are mainly caused by viruses and bacteria by which the most serious diseases are White Spot Disease (WSD), Acute Hepatopancreatic Necrosis Disease (AHPND), Hepatopancreatic Microsporidiosis, Yellow Head Disease, and Infectious Myonecrosis [4].

WSD is a highly lethal shrimp viral disease caused by White Spot Syndrome Virus (WSSV). WSSV is an enveloped, rod-shaped, tailed, and double-stranded DNA virus [5] classified under family Nimaviridae and genus Whispovirus [6]. WSSV had emerged in China since year 1992 and spread to other Asia and America regions [7,8]. This disease can lead to 100% mortality within 3–10 days post-infection [5]. The host range of WSSV includes *P. monodon*, *L. vannamei*, *M. rosenbergii*, and other Penaeid shrimp species. Some clinical signs of WSD are lethargy, white spot formation on muscle, and reduced appetite [5].

In addition, AHPND is a serious shrimp bacterial disease caused by a pathogenic strain of Gram-negative *Vibrio parahaemolyticus* bacteria known as Vp_{AHPND} [9,10]. The Vp_{AHPND} bacteria contain a 70-kbp plasmid (pVA1) capable of producing *Photorhabdus* insect-related (Pir) toxins, PirA and PirB [9]. AHPND had emerged in China since year 2009 which then spread to Southeast Asia and Mexico regions [11,12]. This disease can cause 40–100% mortality within early 35 days shrimp post-stocking [13]. AHPND disease outbreaks had been reported for *P. monodon*, *L. vannamei*, and *Fenneropenaeus chinensis* [14]. The gross clinical signs of AHPND disease include slow growth, lethargy, pale and atrophied hepatopancreas, empty stomach, and empty gut [13]. Intriguingly, despite being susceptible to Vibriosis disease caused by *V. parahaemolyticus* bacteria [15], *M. rosenbergii* under salinity condition of 20 ppt or lower was shown to be not susceptible to AHPND infection [16].

Different strategies are applied in shrimp disease prevention which include selective breeding [17], antibiotics usage [18], probiotics usage [19], and proper biosecurity measures [17]. For selective breeding, it is important to ensure the successful accumulation of desired genetic variants associated with stronger immune response. Among the crucial shrimp innate immune genes, Janus Kinase (JAK)-Signal Transducer and Activator of Transcription (STAT) pathway components can be specially highlighted due to its important and diverse functioning, for example, in immunity [20,21], neuron signalling [22], endocrine [23], stress-induced cell survival [24], and metabolism [25]. JAK-STAT pathway activation involves initial cytokine recognition by the receptor, followed by receptor dimerization, JAK phosphorylation, STAT phosphorylation and dimerization, and lastly translocation of dimerized STAT to the nucleus for gene expression regulation [21,26]. Seven mammalian STATs had been determined, including STAT1, STAT2, STAT3, STAT4, STAT5A, STAT5B, and STAT6 [21]. Although less studied compared to model organisms, shrimp JAK-STAT pathway components such as JAK,

STAT, Suppressors of Cytokine Signalling (SOCS), and Protein Inhibitor of Activated STAT have also been identified through various research efforts in the past years [27–29].

Furthermore, there had been some studies on the STAT gene expression changes in different shrimp species after pathogenic infections. STAT gene expression was up-regulated in *Fenneropenaeus chinensis* challenged with WSSV and *Vibrio anguillarum* [30]. The significant up-regulation of *Marsupenaeus japonicus* [31] and *L. vannamei* [32] STAT gene expressions were identified under WSSV infection. Nevertheless, under some diseased conditions, *Macrobrachium* spp. also demonstrated non-differential STAT gene expression. For example, *M. nipponense* had no significant STAT gene expression changes after *Aeromonas hydrophila* [33] and non-O1 *Vibrio cholerae* [34] bacterial infections. Interestingly, due to the immune signalling importance of STAT gene, there exists risk of shrimp STAT manipulation by the invading pathogens as demonstrated by the shrimp STAT hijacking by WSSV virus [35].

The study of gene expression is an efficient strategy for the fast and accurate determination of gene activation or repression during pathogenic infections. Real time quantitative PCR (qPCR) and RNA-Seq analyses are more commonly utilized for gene expression studies in recent decades [36,37]. qPCR involves the usage of intercalating dyes or probes and qPCR machine for the determination of gene expression fold change between different treatment groups [38]. RNA-Seq utilizes high throughput next-generation sequencing (NGS) technology and has advantages in terms of price, efficiency, difficulty, and application range compared to more traditional methods such as microarray [39].

Despite the increasing numbers of gene expression studies involving pathogen-challenged shrimps, there had been a lack of research focusing on the comparison of immune gene expressions across different pathogenic conditions especially STAT gene. Therefore, this study involved identification and comparison of differential gene expressions of *M. rosenbergii* STAT (*MrST*) and *P. monodon* STAT (*PmST*) upon WSSV and *V. parahaemolyticus*/*Vp_{AHPND}* infections. STAT gene was selected mainly because of its diverse functional importance through JAK-STAT pathway. This was followed by sequence and structure divergence identification between *MrST* and *PmST*. This is because genetic variations can lead to significant gene expression changes and functional alterations during pathogenic infections. A comparative transcriptomic analysis was also conducted to elucidate the underlying stress, endocrine, immune, signalling, and structural DEGs associated with STAT gene functioning during pathogenic infections. Overall, this study had the aim of obtaining more information on the functional importance of shrimp STAT genes involved in the aspects of expression, sequence, structure, and associated genes. The aim was successfully achieved.

2.0 Materials and methods

2.1 Pathogen preparations

For WSSV virus propagation, the feeding of local *P. monodon* shrimps (15–20 g body weight) with WSSV-infected shrimp muscle tissues was conducted. The moribund shrimps were confirmed to be WSSV positive through PCR [40] and stored at -80°C. WSSV virus stock solution was then prepared [41] which involved the homogenization and lysis of the WSSV-infected shrimp muscle tissues in TN Buffer followed by centrifugation, filtration, and storage at -80°C. The WSSV stock solution viral copy number was quantified using primer pairs VP28-140Fw and VP28-140Rv [42].

On the other hand, *P. monodon* suspected with AHPND outbreak were collected and validated through both clinical sign observation and AP3 PCR detection method [43]. The *Vp_{AHPND}* bacteria [44] were selectively propagated by incubating the digestive organs of *Vp_{AHPND}*-infected shrimps in the order of tryptic soy broth (TSB+), thiosulfate citrate bile salt

(TCBS) agar, and tryptic soy agar (TSA+). The bacteria preservation was done through cryovials (CRYOBANK™) at -80°C and utilized for downstream experiments.

2.2 Pre-challenge works

For the WSSV and *V. parahaemolyticus* challenge with *Macrobrachium rosenbergii*, *M. rosenbergii* juvenile prawns (5–8 g body weight) were purchased from a hatchery at Kuala Kangsar, Perak, Malaysia. The acclimatization of the prawns was conducted for seven days under aseptic experimental setup. Each tank contained 10 prawns with aerated freshwater at $28 \pm 1.0^{\circ}\text{C}$.

Whereas for WSSV challenge with *P. monodon*, locally obtained juvenile 4th generation *P. monodon* shrimps (15–20 g body weight) of Mozambique, Africa strain (10 shrimps per tank) were acclimatized for seven days under aseptic experimental setup with aerated artificial seawater (30 ppt) at $28 \pm 1.0^{\circ}\text{C}$. For the Vp_{AHPND} experimental challenge, disease tolerant cross-bred (13th generation Madagascar strain with 5th generation local strain) juvenile *P. monodon* shrimps (15–20 cm body length) were involved. The acclimatization of the shrimps (27 shrimps each tank) was done for seven days under aseptic experimental setup with aerated artificial seawater (30 ppt) at $28 \pm 1.0^{\circ}\text{C}$.

The negative screening of the prepared *M. rosenbergii* and *P. monodon* shrimps was conducted before experimental challenge using PCR methods and confirmed to be WSSV-free [40] and *V. parahaemolyticus*/ Vp_{AHPND} -free [43] respectively.

2.3 Experimental challenge details

The intramuscular injection of *M. rosenbergii* prawns was conducted which involved 100 μl filtered WSSV virus stock solution (1×10^5 copies/ml) (WSSV treatment groups), 100 μl cultured *V. parahaemolyticus* (PCV08-7) (1×10^5 cfu/ml) (*V. parahaemolyticus* treatment groups), and 100 μl 2% NaCl (w/v) (negative control groups) respectively. The shrimp hepatopancreas was collected at 0, 3, 6, 12, 24, and 48 hours post-infection (hpi) and stored at -80°C . The challenge details were described in previous publications [45,46].

Besides that, for the WSSV experimental challenge, *P. monodon* shrimps were injected with 100 μl filtered WSSV stock solution (4.11×10^5 copies/ μl). Sterile PBS was injected for the negative control group shrimps. The shrimp hepatopancreas collection was done at 0, 3, 6, 12, 24, and 48 hpi and also 12 days post-infection (dpi) (survivors) and stored at -80°C . The challenge details were described in previous publication [47].

For the Vp_{AHPND} experimental challenge, *P. monodon* shrimps were infected with Vp_{AHPND} bacteria (KS17.S5-1 positive strain) (2×10^6 cfu/ml) [48] based on a modified immersion method [10]. Sterile TSB+ broth was used instead of Vp_{AHPND} for the negative control group shrimps. The shrimp hepatopancreas was collected at 0, 3, 6, 12, 24, and 48 hpi and stored at -80°C . The challenge details were also described in previous publication [44].

All tanks were equipped with aerators and water filters. The experimental challenges were conducted with three biological replicates for each treatment and control groups. The positive screening of the challenged shrimps was done through PCR methods for WSSV [40] and *V. parahaemolyticus*/ Vp_{AHPND} [43] confirmation respectively. The University of Malaya granted Ethical approval for the study within its facilities (Ethical Application Ref: S/31012019/26112018-05/R).

2.4 Total RNA extraction and first strand cDNA synthesis

Total RNA samples were extracted from shrimp hepatopancreas at each post-infection time interval of both treatment and control groups using NucleoSpin RNA II Extraction Kit (Macherey's-Nagel, Germany), RNA Isolation Kit (Macherey's-Nagel, Germany), and

TransZol Up Plus RNA Kit (TransGen Biotech, Beijing, China) respectively. The extracted RNA samples were also treated with TransScript[®] One-Step gDNA Removal and cDNA Synthesis SuperMix (TransGen Biotech, Beijing, China) to achieve DNA contaminant removal and first strand cDNA synthesis for subsequent downstream applications. The manufacturer's protocols were followed for all kits utilized.

2.5 Expression profile comparison through qPCR analysis

The STAT gene expression profiles of *M. rosenbergii* (*MrST*) and *P. monodon* (*PmST*) during WSSV and *V. parahaemolyticus*/*Vp*_{AHPND} infections were determined and compared through quantitative real-time PCR (qPCR) analysis. Three biological replicates with three technical replicates each were applied for every treatment group. The qPCR primers were designed through PrimerQuest Tool software (<https://sg.idtdna.com/Primerquest/home/Index>) and listed in [S1 Table](#).

The *MrST* qPCR experiments were conducted using TaqMan[®] Universal PCR Master Mix kit and Step One Plus Real-Time PCR System[®] instrument (Applied Biosystems, Foster City, CA, USA). The qPCR reaction (20 μ l) consisted of 10 μ l TaqMan Universal RT-PCR Master Mix, 1 μ l primers/probe set containing 900 nM of forward reverse primers, 300 nM probe, 2 μ l template cDNA, and nuclease-free water. The qPCR cycling program involved 50°C for 2 mins, 40 cycles of 95°C for 10 mins, 95°C for 15 secs, and 60°C for 1 min. Elongation factor 1-alpha (*EF1a*) gene was chosen as the internal control reference gene [49]. The experimental protocol details were mentioned previously [50].

The *PmST* qPCR experiments were carried out using GoTaq[®] qPCR Master Mix kit (Promega, Madison, Wisconsin, USA) and Agilent Technologies Stratagene Mx3005P instrument. The qPCR reaction (20 μ l) included 10 μ l GoTaq[®] qPCR 2X Mix, 500 nM forward primer, 500 nM reverse primer, 2 μ l template cDNA, and nuclease-free water. The qPCR cycling program of 95°C for 2 mins, 40 cycles of 95°C for 15 s, and 56°C for 35 secs was utilized. *EF1a* gene was selected as the internal control reference gene as well.

The analysis of the Ct values obtained was conducted through Livak's 2^{- Δ ddCt} relative quantification method [51]. The differential gene expression values determined were then statistically validated through One-Way ANOVA analysis with post hoc Duncan test using SPSS software Version 22 (Significance value: P<0.05). The post hoc Duncan test was carried out to identify the exact differences of different treatment groups (classified under alphabetical subsets) when One-Way ANOVA analysis was significant. The raw data for the qPCR experiments was shown in [S1 Data](#).

2.6 Sequence and structural comparison of STAT genes

The *MrST*, *PmST*, and *LvST* sequences were retrieved from NCBI nucleotide database (NCBI Accession Numbers: **KT380661.1**; **AY327491.1**; **HQ228176.1**) [46]. The *MrST* sequence validation was done through PCR method and subsequent Sanger Sequencing analysis. In addition, the *PmST* sequence of disease tolerant *P. monodon* shrimps used in this study was determined through PCR technique using conserved site targeting strategy. The PCR primers involved were designed using PrimerQuest Tool software (<https://sg.idtdna.com/Primerquest/home/Index>) and listed in [S2 Table](#). The PCR experiments were conducted using GoTaq[®] Flexi DNA Polymerase kit (Promega, Madison, Wisconsin, USA) and Eppendorf Mastercycler EP Gradient S instrument. Each PCR reaction contained 5 μ l 5 x GoTaq[®] Flexi Buffer, 1.5 μ l 25 mM MgCl₂ solution, 0.5 μ l 10 mM dNTPs, 0.25 μ l GoTaq[®] DNA Polymerase (5U/ μ l), 400 nM forward primer, 400 nM reverse primer, 1.2 μ l template cDNA, and nuclease-free water.

The PCR cycling program involved initial denaturation of 95°C for 5 mins, 40 cycles of 95°C for 45 s, 56.7°C for 45 s and 72°C for 45 s, and final extension of 72°C for 5 mins.

The amplified PCR products were then sent for Sanger Sequencing. The sequencing results were trimmed using MEGA7 [52] and Chromas (<https://technelysium.com.au/wp/chromas/>) software. The sequence identities and their homologs were confirmed through NCBI homology BLAST search [53]. The translated amino acid sequences of MrST and PmST were obtained using NCBI Open Reading Frame (ORF) Finder (<https://www.ncbi.nlm.nih.gov/orffinder/>), ExpASY Translate (<https://web.expasy.org/translate/>), and Show Translation (https://www.bioinformatics.org/sms/show_trans.html). The MrST, PmST, PmST (disease tolerant strain), and LvST nucleotide and translated amino acid sequences were compared using Clustal Omega software. The MrST, PmST, LvST, and other STAT homologous sequences (retrieved from NCBI database) were utilized for phylogenetic analysis at nucleotide and amino acid levels (Maximum likelihood method) through MEGA7 software [52]. For structural comparison, the MrST and PmST (disease tolerant strain) translated amino acid sequences were characterized and compared *in silico* using ProtParam (<https://web.expasy.org/protparam/>), NCBI Conserved Domain Search (CDD) [54], Protter [55], MultiLoc 2 Predictor [56], RNAFold Web Server [57], PSIPRED [58], PROSITE [59], and SWISS-MODEL [60].

2.7 Identification and comparison of annotated differentially expressed genes (DEGs)

For additional identification and validation of STAT-related functional genes, the determination and comparison of Differentially Expressed Genes (DEGs) from *M. rosenbergii* and *P. monodon* under WSSV and *V. parahaemolyticus*/*Vp_{AHPND}* infection conditions were conducted. The DEGs involved were identified and retrieved from RNA-Seq results of associated previous publications [44–47]. The data is available at the NCBI SRA database: **SRR1424572**, **SRR1424574**, **SRR1424575**, and **SRP153251**.

Generally, the extracted *M. rosenbergii* and *P. monodon* hepatopancreas RNA samples were treated with DNase and subsequently sent for cDNA library preparation and NGS sequencing using Illumina HiSeq 2000/BGI-SEQ 500 Sequencer platform by the Beijing Genome Institute (Hong Kong). The raw sequencing reads were filtered by which the clean reads were used for DEGs determination. This was followed by the functional annotation of the identified DEGs through mapping to different databases. The details of RNA-Seq data analysis were described in previous publications [44–47].

The stress, immune, and endocrine DEGs were mainly identified and compared between different treated samples. The patterns of interaction including co-activation or co-repression of DEGs under different pathogenic conditions especially those involved in STAT functioning were elucidated. The qPCR validation details of these RNA-Seq results were also described in previous publications [44–47].

3.0 Results

3.1 Differential expression profiles between *M. rosenbergii* STAT (*MrST*) and *P. monodon* STAT (*PmST*) during pathogenic infections

The relative gene expression fold changes of *MrST* [50] and *PmST* (disease tolerant strain) across different post-infection time points of WSSV and *V. parahaemolyticus*/*Vp_{AHPND}* infections were determined and compared as shown in Fig 1. The individual treatment condition

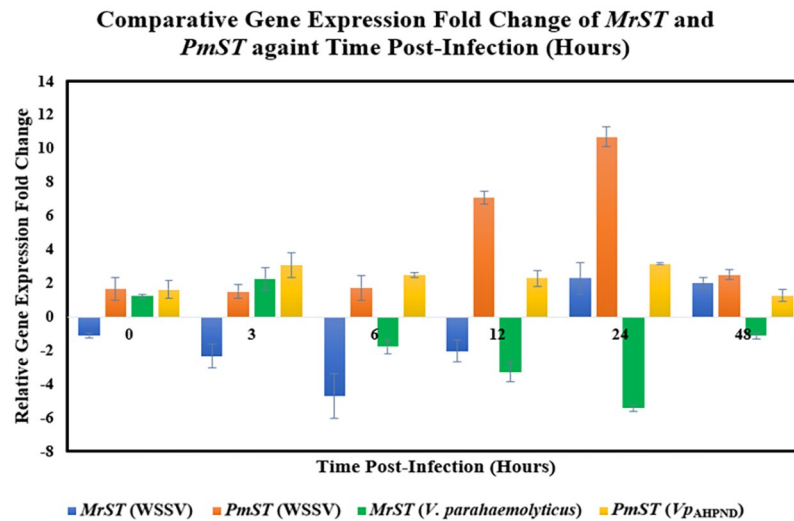


Fig 1. Comparative gene expression fold change of *MrST* and *PmST* against time post-infection (hours) (WSSV and *V. parahaemolyticus/VpAHPND*). All relative gene expression fold changes were statistically significant ($P < 0.05$). The error bars indicated standard deviations of the data. [*MrST* (WSSV) Fold changes: 0 hpi: -1.113; 3 hpi: -2.332; 6 hpi: -4.699; 12 hpi: -2.038; 24 hpi: 2.287; 48 hpi: 2.017]. [*PmST* (WSSV) Fold changes: 0 hpi: 1.650; 3 hpi: 1.500; 6 hpi: 1.729; 12 hpi: 7.082; 24 hpi: 10.691; 48 hpi: 2.510]. [*MrST* (*V. parahaemolyticus*) Fold changes: 0 hpi: 1.238; 3 hpi: 2.272; 6 hpi: -1.766; 12 hpi: -3.262; 24 hpi: -5.429; 48 hpi: -1.125]. [*PmST* (*VpAHPND*) Fold changes: 0 hpi: 1.622; 3 hpi: 3.059; 6 hpi: 2.500; 12 hpi: 2.298; 24 hpi: 3.139; 48 hpi: 1.273].

<https://doi.org/10.1371/journal.pone.0258655.g001>

gene expression fold changes and statistical validations were provided in S1–S4 Figs and S3–S6 Tables.





By referring to Fig 1, during WSSV infection, *MrST* gene expressions were initially down-regulated with the greatest down-regulation detected at 6 hpi, followed by slight up-regulations at 24 and 48 hpi. Whereas *PmST* gene expressions were generally up-regulated with sharp up-regulation at 12 hpi and highest peak at 24 hpi. On the other hand, in response to bacterial (*V. parahaemolyticus/VpAHPND*) infections, *MrST* gene expressions demonstrated slight up-regulation at 3 hpi followed by down-regulation from 6 hpi to 48 hpi with the lowest point at 24 hpi. *PmST* gene expressions showed significant up-regulation at 3 hpi, which was maintained until 24 hpi, and reverted to normal at 48 hpi. Intriguingly, *MrST* gene expressions were significantly down-regulated during both viral (early post-infection time points) and bacterial (later post-infection time points) infections compared to the significantly up-regulated *PmST* gene expressions.

3.2 Sequence comparison between *MrST*, *PmST*, and *L. vannamei* STAT (*LvST*)

Several selected shrimp STAT complete cds sequences, *MrST* (Accession Number: **KT380661**), *PmST* (disease tolerant strain), *PmST* (Accession Number: **AY327491.1**), and *LvST* (Accession Number: **HQ228176.1**) were obtained and compared using Clustal Omega software at translated amino acid (Fig 2) and nucleotide (S5 Fig) levels. The important conserved and diverged sites between the aligned sequences were marked by which a significant number of diverged sites were located at the 5' UTR and 3' UTR regions.

At nucleotide level, the major conserved area was found at the middle region whereas long conserved overlaps were more frequently identified at the start and end regions. Important diverged sites determined between *PmST* (disease tolerant strain) and *PmST* (**AY327491.1**)

MrST	MSPNKVGIEAKVKTTMSLNRAAQLPQDALRQVQIVVNEQFP I EVRH YLAGNIEEKIQW	60
LvST	-----MSLNRAAQLPPXDLRRVGIYGEQFP I EVRH YLAWNIEDKMQW	45
PmST (New)	-----MSESTMSLNRAAQLPADDLRRVGGIYGEQFP I EVRH YLAGNIEDKMQW	50
PmST (AY327491.1)	-----MSESTMSLNRAAQLPADDLRRVGGIYGEQFP I EVRH YLAGNIEDKMQW	50
MrST	NEIDPDNPAHSQYAHTIVSQLIQEMENKSLSYVNNEDLFLVRMRLNEANLFKTRYLNTN	120
LvST	NEIDPDNPSHTQYQSLSVQLIQEIEENKALSYANNEDLFLVRMRLDEAATSFRTRYLNSN	105
PmST (New)	NEIDPDNPSHSQYAQSLSVQLIQEIEENKALSYANNEDLFLVRMRLDEAATSFRTRYLNSN	110
PmST (AY327491.1)	NEIDPDNPSHSQYAQSLSVQLIQEIEENKALSYANNEDLFLVRMRLDEAATSFRTRYLNSN	110
MrST	PLALVSIIRNCLNTEHLVQVHESMLGIVGPGVNMIVEPCTEIVQELVLRHRTRETAD	179
LvST	PLGLVGIIRQCLNTEHLVQVQENMLGGVSHATNMVIEPCAEIEQELRIHLHRTRETAN	165
PmST (New)	PLGLVGIIRQCLNTEHLVQVQENMLGGVSHATNMVIEPCAEIEQELRIHLHRTRETAN	170
PmST (AY327491.1)	PLGLVGIIRQCLNTEHLVQVQENMLGGVSHATNMVIEPCAEIEQELRIHLHRTRETAN	170
MrST	ELRQLEQEESFALQYHDCAKINAHLSHIQSQERTQNRDVENMLRKRKEVGEQQLAQV	239
LvST	ELRHLEQEESFALQYHDCAKINAHLSHIQSQERTQNRREMEQSLRRRKLGEQQLAQV	225
PmST (New)	ELRHLEQEESFALQYHDCAKINAHLSHIQSQERTQNRREMEQSLRRRKLGEQQLAQV	230
PmST (AY327491.1)	ELRHLEQEESFALQYHDCAKINAHLSHIQSQERTQNRREMEQSLRRRKLGEQQLAQV	230
MrST	SGLLQRRMALAEKHKGTIDRLNSLQQRILDEELINWIKREQQMAGNGRPFNQKLDQIQEW	299
LvST	SGLLQLRMALADKHKGTIDRLNSLQQRILDEELINWIKRDQMHGNGKPFNPNKLDQIQEW	285
PmST (New)	SGLLQLRMALADKHKGTIDRLNSLQQRILDEELINWIKRDQMHGNGKPFNPNKLDQIQEW	290
PmST (AY327491.1)	SGLLQLRMALADKHKGTIDRLNSLQQRILDEELINWIKRDQMHGNGKPFNPNKLDQIQEW	290
MrST	CEALAEIWLNRHQIKECERHQT K IPIAPPGGVDMLPTLNSHITRLSSSLVSTFIIIEKQ	359
LvST	CEALAEIWLNRHQIKECERHQT K IPIAPPGGVDMLPTLNSHITRLSSSLVSTFIIIEKQ	345
PmST (New)	CEALAEIWLNRHQIKECERHQT K IPIAPPGGVDMLPTLNSHITRLSSSLVSTFIIIEKQ	350
PmST (AY327491.1)	CEALAEIWLNRHQIKECERHQT K IPIAPPGGVDMLPTLNSHITRLSSSLVSTFIIIEKQ	350
MrST	PPQVMKTNTFRFATVRLLVGGKLNVMHTPPQVRVSIIEAQANALLKNDQMNKGEQSGEI	419
LvST	PPQVMKTNTFRFATVRLLVGGKLNVMHTPPQVRVSIIEAQANALLKNDQMNKGEQSGEI	405
PmST (New)	PPQVMKTNTFRFATVRLLVGGKLNVMHTPPQVRVSIIEAQANALLKNDQMNKGEQSGEI	410
PmST (AY327491.1)	PPQVMKTNTFRFATVRLLVGGKLNVMHTPPQVRVSIIEAQANALLKNDQMNKGEQSGEI	410
MrST	LNNTGTMEYHQGT RQLSVSFRIMQLRKIKRAEKKGTESVMDEKFSLLFQSQF SVGGGELV	479
LvST	LNNTGTMEYHQGT RQLSVSFRIMQLRKIKRAEKKGTESVMDEKFSLLFQSQF SVGGGELV	465
PmST (New)	LNNTGTMEYHQGT RQLSVSFRIMQLRKIKRAEKKGTESVMDEKFSLLFQSQF SVGGGELV	470
PmST (AY327491.1)	LNNTGTMEYHQGT RQLSVSFRIMQLRKIKRAEKKGTESVMDEKFSLLFQSQF SVGGGELV	470
MrST	FQWVTLSLPVVVI VHGNDQEPHAWATVSWDNFAEQGRIPFTVPEKVPWPQIAEMLDTKFK	539
LvST	FQWVTLSLPVVVI VHGNDQEPHAWATVSWDNFAEQGRIPFTVPEKVPWPQIAEMLDTKFK	525
PmST (New)	FQWVTLSLPVVVI VHGNDQEPHAWATVSWDNFAEQGRIPFTVPEKVPWPQIAEMLDTKFK	530
PmST (AY327491.1)	FQWVTLSLPVVVI VHGNDQEPHAWATVSWDNFAEQGRIPFTVPEKVPWPQIAEMLDTKFK	530
MrST	AATGRGLTEDNLKFLAGKAFRLDSVQVQDFTNMMLSHSQFCKEPLSERNFTFWWEFFAVM	599
LvST	AATGRGLTEDNLKFLAGKAFRL--POVQDFTNMMLSHSQFCKEPLSERNFTFWWEFFAVM	583
PmST (New)	AATGRGLTEDNLKFLAGKAFRL--POVQDFTNMMLSHSQFCKEPLSERNFTFWWEFFAVM	588
PmST (AY327491.1)	AATGRGLTEDNLKFLAGKAFRL--POVQDFTNMMLSHSQFCKEPLSERNFTFWWEFFAVM	588
MrST	KVTRHRLRQVINDGSIMGFVGRRAEEMLNKNSKSGTFLLRFSOSELGGVTIAWPHYEDTTK	659
LvST	KVTRHRLRQVINDGSIMGFVGRRAEEMLNKNSKSGTFLLRFSOSELGGVTIAWPHYEDTTK	643
PmST (New)	KVTRHRLRQVINDGSIMGFVGRRAEEMLNKNSKSGTFLLRFSOSELGGVTIAWPHYEDTTK	648
PmST (AY327491.1)	KVTRHRLRQVINDGSIMGFVGRRAEEMLNKNSKSGTFLLRFSOSELGGVTIAWPHYEDTTK	648
MrST	GDQRDVFMLQPF TSKAF AIRPLADVIADLKYLLYL YPNVPKQAF GKYYTPMGGEQPTTN	718
LvST	ACQRDVFMLQPF TSKAF AIRPLADVIADLNYLLYL YPNVPKQAF GKYYTPMGGEQPTTN	703
PmST (New)	ACQRDVFMLQPF TSKAF AIRPLADVIADLNYLLYL YPNVPKQAF GKYYTPMGGEQPTTN	708
PmST (AY327491.1)	ACQRDVFMLQPF TSKAF AIRPLADVIADLNYLLYL YPNVPKQAF GKYYTPMGGEQPTTN	708
MrST	NGYVKPHLITHVPGWSVAAGSHDSYPNTPQPMYRPHDSHMGDPPSVSSNPSDCVSTMPPY	778
LvST	NGYVKPQLKTHVPGWS--GDPHDSYPNTPQPMYR--GMDPPSVSSNPSDCVSTVPTY	757
PmST (New)	NGYVKPQLKTHVPGWS--GDPHDSYPNTPQPMYR--GMDPPSVSSNPSDCVSTDQKP	762
PmST (AY327491.1)	NGYVKPQLKTHVPGWS--GDPHDSYPNTPQPMYR--GMDPPSVSSNPSDCVSTDQKP	762
MrST	--NDTDVPILENLPD TDFDINLDFLQTNFMKPKQ	811
LvST	--NECEYDQFLENLSEADFPDMNDFLQTNFMKPKQ	790
PmST (New)	TLDSPLFDA--ANVLSDFS-----	779
PmST (AY327491.1)	TLDSPLFDA--ANVLSDFS-----	779

Fig 2. Sequence comparison of MrST, LvST, PmST (New) (disease tolerant strain), and PmST (Accession number: AY327491.1) translated amino acid sequences. * represents common conserved sites between all sequences.  represents important long conserved overlaps between all sequences.  represents important divergent sites between PmST (cross-bred disease tolerant strain) and PmST (Accession number: AY327491.1).  represents important divergent sites between MrST and other STAT sequences.  represents important amino acid addition or deletion between MrST and other STAT sequences.

<https://doi.org/10.1371/journal.pone.0258655.g002>

included 4, 11, 42, 179, 335, 1268, 1959, 1991, 2004, 2487, 2488, 2489, and 2491 bp. Nucleotide additions or deletions of *MrST* sequence compared to other STAT sequences were mainly identified at the regions of 16–17, 33, 56–57, 81–82, 108–110, 1786–1791, 2256–2257, and 2310–2315 bp. The major nucleotide diverged sites of *MrST* sequence compared to other STAT sequences were concentrated at the 5' UTR, 307, 478, 730, 770, 977, 1224, 1780, 1926, 1995, 2011, 2081, 2172, 2240, 2280, and 2367 bp regions.

Besides that, at translated amino acid level, both major conserved area and long conserved overlaps between compared STAT sequences were located at the middle region. Despite the multiple important diverged sites identified between the two compared *PmST* nucleotide sequences, at amino acid level, only two amino acid alterations were discovered at positions of 614 aa [K (Lysine) to E (Glutamic Acid)] and 629 aa [F (Phenylalanine) to V (Valine)] from *PmST* (AY327491.1) to *PmST* (disease tolerant strain) respectively. Amino acid additions or deletions of *MrST* sequence compared to other STAT sequences were determined at the regions of 147–148, 562–563, 717–718, 735–736, and 753–756 aa. The major amino acid diverged sites of *MrST* sequence compared to other STAT sequences were located at the 35, 75, 110, 150, 215, and 429 aa regions. Interestingly, aligned *MrST* and *LvST* sequences had overlapping stop codon positions.

Homologous STAT amino acid sequences of *MrST* were determined through NCBI homology protein BLAST search, which included *F. chinensis* (89%), *Scylla paramamosain* (88%), *Eriocheir sinensis* (87%), *L. vannamei* (87%), *Marsupenaeus japonicus* (86%), and *Cryptotermes secundus* (69%). Whereas for *PmST* amino acid sequence, the homologous STAT amino acid sequences identified were *L. vannamei* (99%), *F. chinensis* (99%), *M. japonicus* (95%), *Portunus trituberculatus* (87%), *S. paramamosain* (86%), *E. sinensis* (85%), and *Armadillidium nasatum* (67%).

In addition, the phylogenetic analyses of *MrST*, *PmST*, and homologous STAT nucleotide and amino acid sequences were shown in [S6A and S6B Fig](#). The *PmST* nucleotide sequence was most closely related to *F. chinensis* STAT, followed by *L. vannamei* STAT, *M. japonicus* STAT, and finally *MrST* nucleotide sequences within the same evolutionary clade compared to other 10 homologous STAT nucleotide sequences ([S6A Fig](#)). Whereas the *PmST* amino acid sequence had the closest relationship to *L. vannamei* STAT, followed by *F. chinensis* STAT, *M. japonicus* STAT, and *MrST* amino acid sequences within the same evolutionary clade ([S6B Fig](#)).

3.3 *In silico* structural comparison between *MrST* and *PmST* sequences

A full-length complete cds *PmST* (disease tolerant strain) nucleotide sequence of 2491 bp was obtained through PCR, Sanger Sequencing, sequence alignment, and trimming. *In silico* structural characterization was then conducted using the 2906 bp *MrST* (Accession Number: **KT380661**) and 2491 bp *PmST* (disease tolerant strain) nucleotide sequences.

Based on the analysis results of NCBI ORF Finder, ExpASY Translate, Show Translation, ProtParam, and NCBI CDD, *MrST* nucleotide sequence had an ORF region of 2436 bp out of the total 2906 bp ([S7A Fig](#)) encoding for a 811 aa long protein ([S7B Fig](#)) with theoretical isoelectric point of 6.04 and molecular mass of 93 kDa. On the other hand, a 2340 bp ORF region was determined from the 2491 bp *PmST* nucleotide sequence ([S8A Fig](#)) encoding for a 779 aa long protein ([S8B Fig](#)). This translated amino acid sequence had theoretical isoelectric point of 6.11 and molecular mass of 89 kDa. Four functional conserved domains were identified from the *MrST* and *PmST* protein sequences, which included STAT_int domain (protein interaction) (17 aa-141 aa; 7 aa-133 aa), STAT5_CCD domain (coiled-coil) (159 aa-352 aa; 150 aa-343

aa), STAT_bind domain (DNA binding) (354 aa-603 aa; 345 aa-592 aa), and SH2 domain (Src homology 2) (594 aa-710 aa; 583 aa-699 aa) respectively (S9A and S9B Fig).

Both MrST and PmST protein sequences were predicted to be intracellular and non-transmembrane through Protter analysis. MrST and PmST proteins had high probabilities to be located within cytoplasmic region (estimated probability of 0.61) and nuclear region (estimated probability of 0.94) respectively based on the MultiLoc 2 prediction analysis. The secondary structures of MrST and PmST protein sequences were predicted as shown in S10A and S10B Fig. For MrST protein sequence, 23 high probability common motifs and 1 Src homology 2 (SH2) domain profile (probability score, 13.148) were found (S11A Fig). Whereas 25 high probability common motifs and 1 SH2 domain profile (probability score, 13.519) were matched to PmST protein sequence (S11B Fig). 3D protein structures of MrST and PmST protein sequences were predicted which contained α -helix, β -sheet, and coil structures (S12A and S12B Fig). The optimal model template used for both structures was *Homo sapiens* STAT 5A (PDB ID: 1y1u1.A) (QMEAN: -2.04; -2.44).

3.4 Comparative transcriptomic differentially expressed genes (DEGs) analysis

The important stress, endocrine, immune, signalling, and structural DEGs of *M. rosenbergii* and *P. monodon* during WSSV and *V. parahaemolyticus*/*Vp*_{AHPND} infections were identified and compared in the Fig 3 below. More details including gene identities, differential expression values, and annotation sources were given in the S7 Table.

Based on Fig 3, a significant higher number of up-regulated DEGs compared to down-regulated DEGs can be observed. *M. rosenbergii* treatment groups had more up-regulated DEGs

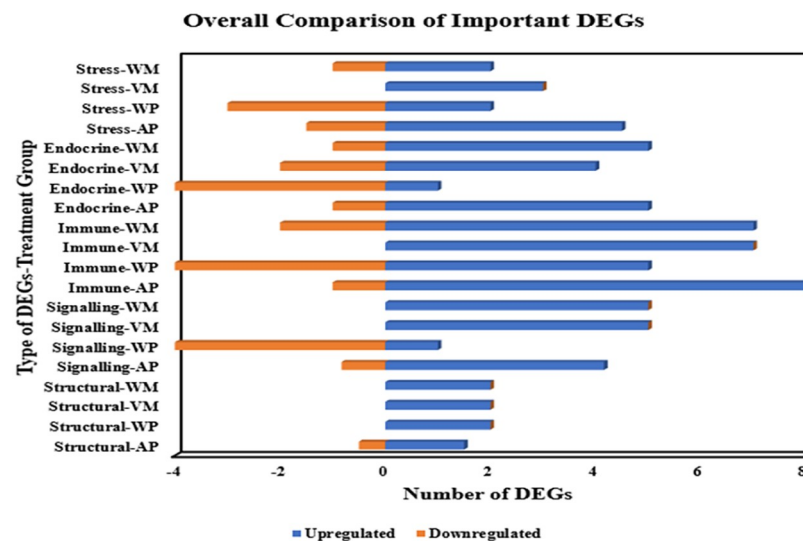


Fig 3. Overall comparison of important DEGs involving type of DEGs-treatment group and number of DEGs. Treatment Groups: WM: WSSV-infected *M. rosenbergii*; VM: *V. parahaemolyticus*-infected *M. rosenbergii*; WP: WSSV-infected *P. monodon* at 12 dpi; AP: *Vp*_{AHPND}-infected *P. monodon*. Stress DEGs: Inositol 1,4,5-trisphosphate receptor, Dopamine N-acetyltransferase, Hsp90, Apoptosis-stimulating of p53 protein 1, Caspase, Apoptosis-inducing factor (AIF). Endocrine DEGs: Mitochondrial coenzyme A transporter, ATP binding cassette transmembrane transporter, Trehalose transporter, Polysaccharide lyase, Trypsin, Peroxisomal acyl-coenzyme A oxidase. Immune DEGs: Transglutaminase, C-type Lectin, HMGB, ALF1, ALF3, proPO, Superoxide Dismutase, Glutathione Peroxidase, Catalase. Signalling DEGs: Ceramide synthase, Calcium-activated chloride channel regulator, Inward rectifier potassium channel, STAT, IMD, TBK1. Structural DEGs: Actin, Ankyrin.

<https://doi.org/10.1371/journal.pone.0258655.g003>

compared to *P. monodon* treatment groups. WP group possessed higher number of down-regulated DEGs compared to other treatment groups. Some DEGs were only down-regulated in WP group involving inositol 1,4,5-trisphosphate receptor, apoptosis-stimulating of p53 protein 1, mitochondrial coenzyme A transporter, polysaccharide lyase, trypsin, C-type Lectin, proPO, ceramide synthase, STAT, and TBK1. Intriguingly, Hsp90, transglutaminase, ALF1, ALF3, and ankyrin demonstrated sole up-regulation pattern across all treatment groups. Peroxisomal acyl-coenzyme A oxidase and catalase were up-regulated in *M. rosenbergii* treatment groups while down-regulated in *P. monodon* treatment groups. On the other hand, trehalose transporter was down-regulated in *M. rosenbergii* treatment groups while up-regulated in *P. monodon* treatment groups. Moreover, dopamine N-acetyltransferase and HMGB only showed up-regulation pattern in *P. monodon* treatment groups. Apoptosis-inducing factor (AIF) and IMD were only differentially expressed in *Vp*_{AHPND}-infected treatment group. Caspase was down-regulated in all treatment groups except being up-regulated in VM group.

4.0 Discussion

4.1 Differential gene expression pattern of *MrST* and *PmST* during WSSV and *V. parahaemolyticus/Vp*_{AHPND} infections

STAT gene was chosen for gene expression analyses involving different pathogenic-challenged treatment groups because of its highly diverse gene functioning in the JAK-STAT signalling pathway which possesses stress, endocrine, and immune importance [20,21,23].

Unlike the potential up-regulation of STAT gene expressions in the early WSSV post-infection time points associated with previously described hijacking mechanism adapted by WSSV for viral replication [35], the *MrST* gene expressions were down-regulated in the early WSSV post-infection time points (Fig 1) of this study. This infers that *MrST* was negatively regulated during initial WSSV infection for viral hijacking prevention. There exists possibility of miRNA involvement in such gene regulation which can be postulated based on previously identified down-regulation of human furin gene expression by miR-24 to prevent H5N1 influenza A viral spread [61]. The subsequent upregulation of *MrST* gene expressions at 24 hpi and 48 hpi matched the post-WSSV infection STAT gene expression pattern of VP28 oral-vaccinated *P. monodon* [62]. Based on that gene expression pattern, the continual up-regulation of *MrST* gene expressions after 48 hpi can be inferred. This suggests the significance of *MrST* gene expression and functioning in the strong immune response of *M. rosenbergii* activated in response to WSSV infection similar to the improved immune response of oral-vaccinated *P. monodon*.

Intriguingly, elevated STAT gene expressions caused by VP28 vaccination also aided in lowering viral gene expression and thus slowed down WSSV establishment in WSSV-infected *P. monodon* juvenile [63]. This infers a competitive relationship between host STAT gene expression and WSSV viral gene expression. Hence, the up-regulation of *PmST* gene expressions from 3 hpi to 48 hpi in response to WSSV infection (Fig 1) in this study is suggested to be the collective effect of stronger immune response from disease-resistant *P. monodon* and WSSV viral hijacking.

On the other hand, for *V. parahaemolyticus* infection, the down-regulation pattern of *MrST* gene expressions observed (Fig 1) is supported by a similar scenario of down-regulated STAT gene expressions at later hpi of *V. parahaemolyticus*-infected *S. paramamosain* [64]. The up-regulated *PmST* gene expressions identified in response to AHPND infection (Fig 1) was inferred to be caused by activated *P. monodon* antibacterial immune response similar to the involvement of JAK-STAT pathway in the *M. japonicus* antibacterial immune response [65].

Similar scenario was also reported previously for up-regulated STAT gene expressions in *V. anguillarum*-challenged *F. chinensis* shrimps [30].

4.2 Important conservation and divergence between STAT sequences

The vital conserved areas determined between MrST, PmST (disease tolerant strain), PmST (AY327491.1), and LvST sequences (nucleotide and amino acid) can be applied in cross-species conserved primer development. This is exemplified by the development of conserved primers for decapod crustaceans (including shrimps) [66] and different bear species [67] for mitochondrial genome sequencing purpose. A probable common ancestry is inferred between MrST and LvST based on their overlapping stop codon positions at nucleotide level. This is supported by another inference of a single common ancestor origination for ALF genes of all crustaceans [68]. MrST sequence was most diverged from other compared STAT sequences at nucleotide (S5 Fig) and amino acid (Fig 2) levels. The differential gene expressions between MrST and PmST (Fig 1) might be significantly influenced by these genetic sequence (nucleotide and amino acid) variations involving divergence, additions or deletions. The important effect of genetic variations on the gene expressions had been highlighted by previous works [69,70].

Moreover, the two amino acid changes (614 aa and 629 aa) detected between PmST sequences compared could be essential in the enhanced functioning of PmST in disease tolerant *P. monodon*. These amino acid changes are caused by nonsynonymous mutations. The key outcome of such amino acid changes can be inferred to be the improvement or alteration of PmST protein recognition ability or binding affinity which can be related to some previous research findings [71–73]. The divergence at the 5' UTR and 3' UTR regions of the aligned STAT sequences suggests the potential involvement of pre- or post-transcriptional regulatory elements found in these regions in causing differential gene expressions and alternative disease tolerance. This is validated by previously determined significant correlation between increased gene expression and adaptive evolution in the 3' UTR and amino acid sequence [74].

By referring to the NCBI BLAST search results, although being closely related to shrimp species (*F. chinensis*) (89%), MrST amino acid sequence was also strongly conserved with crab species (*S. paramamosain* and *E. sinensis*) (88%; 87%). This is supported by the close evolutionary relationship between MrST and crab species (*S. paramamosain* and *E. sinensis*) in the phylogenetic analyses conducted (S6A and S6B Fig). Intriguingly, PmST amino acid sequence had high homology to *P. trituberculatus* (87%) in the NCBI BLAST search. This is supported by a previously determined mitochondrial DNA similarity between *P. monodon* and *P. trituberculatus* [75]. Furthermore, there was a close clustering between *Macrobrachium* prawns and Penaeidae shrimps (*P. monodon*, *F. chinensis*, and *L. vananmei*) in the phylogenetic analyses (S6A and S6B Fig), which suggests a similar ancestry between them.

4.3 *In silico* predicted MrST and PmST structural variations

The MrST protein sequence possessed slightly lower theoretical isoelectric point (pI) (6.04) compared to PmST protein sequence (6.11). The subcellular localization prediction of MrST and PmST proteins with intracellular and non-transmembrane properties was determined to be within the cytoplasmic ($P = 0.61$) and nuclear ($P = 0.94$) regions respectively. This is validated by a previously identified correlation of protein pI with subcellular localization by which cytoplasmic region contains higher number of acidic proteins compared to nuclear region [76]. Besides that, the four functional conserved domains (STAT_int, STAT5_CCD, STAT_bind, and SH2) identified for both MrST and PmST protein sequences successfully contributed to the STAT gene identity validation of these sequences. The two amino acid changes

described in Section 3.2 were found within the SH2 conserved domain which has functional importance in STAT dimerization and signalling specificity [77].

4.4 Additional transcriptomic insight into functional DEGs

Based on the transcriptomic DEGs displayed in Fig 3 and S7 Table, further understanding was obtained for the DEGs' functionalities particularly those related to STAT. This is important due to the insufficient number of previous studies on the direct comparison between the transcriptomic DEGs of *M. rosenbergii* and *P. monodon* under viral and bacterial infection conditions. Overall, the significantly higher number of up-regulated DEGs compared to down-regulated DEGs is postulated to be the effect of host immune response activation during pathogenic infection. In addition, the higher number of up-regulated DEGs identified in *M. rosenbergii* compared to *P. monodon* can be correlated to its stronger immune response. Such strong immune response was previously demonstrated by the ability of adult *M. rosenbergii* to achieve clearance of WSSV virus compared to susceptible *P. monodon* [78]. Intriguingly, some down-regulated DEGs were uniquely found in the WP group which resulted in its relatively higher number of down-regulated DEGs among the compared treatment groups. This is postulated to be caused by the decreased host response of survived *P. monodon* after successful WSSV clearance.

The functioning of stress DEGs in the early stress-induced immunoendocrine response is inferred based on both up-regulation of these DEGs in this study and previous publications [79–82]. The up-regulation of endocrine DEGs across different treatment groups is postulated to be the effect of higher energy needs for host immune response activation and post-infection cell repair. This is validated by the significance of energy balance for stress adaptation and aquatic animal tolerance highlighted in previous publications [83,84]. The activated shrimp immune response led to the up-regulation of immune and signalling DEGs. The up-regulation of structural DEGs suggests the high probability of cell and tissue structural repair across different post-infection time points. This is supported by the identification of structural DEGs (including actin-associated genes) with cytoskeleton functions in *V. parahaemolyticus*-infected *L. vannamei* [85]. All these DEGs with stress, endocrine, immune, signalling, and structural functionalities are vital in the overall host response against invading pathogens.

Moreover, the DEGs involved in overall STAT functioning through JAK-STAT pathway include inositol 1,4,5-trisphosphate receptor (associated with intracellular calcium concentration and bradykinin hormonal activation) [86,87], hsp90 (cell proliferation and protein folding) [88–90], caspase (apoptosis) [91], ATP binding cassette transmembrane transporter (cholesterol efflux) [92], C-type Lectin (pathogen recognition) [93], HMGB (inflammatory effect; DAMP) [94,95], ALF1, ALF3 (antimicrobial activity) [28,96], superoxide dismutase, glutathione peroxidase, catalase (antioxidation activity) [97–99], and TBK1 (SOCS-mediated degradation) [100].

Besides that, other DEGs possibly or indirectly associated with JAK-STAT signalling are apoptosis-stimulating of p53 protein 1 (apoptosis) [101–103], apoptosis-inducing factor (AIF) (apoptosis) [104,105], trehalose transporter (cell proliferation) [106], trypsin (viral immune response) [107], peroxisomal acyl-coenzyme A oxidase (associated with leptin and adiponectin; apoptosis) [108,109], transglutaminase (clotting reaction during viral infection) [110], proPO (proPO activation system and melanization) [110], calcium-activated chloride channel regulator (STAT regulation of mucus production) [111,112], and IMD (another important signalling pathway component of invertebrate immune response) [113]. The remaining DEGs may have functional relevance to JAK-STAT signalling pathway, but further validations are needed due to the lack of previous studies.

Interestingly, the uniquely up-regulated DEGs, including peroxisomal acyl-coenzyme A oxidase, catalase, and TBK1 in *M. rosenbergii* infer their greater importance in *M. rosenbergii* host response. On the other hand, dopamine N-acetyltransferase, trehalose transporter, and HMGB showed unique up-regulation in *P. monodon* during pathogenic infections, which suggests their stronger importance in *P. monodon* host response as well. The special functional importance of AIF and IMD signalling pathway in AP group may be further investigated to gain deeper understanding into their sole differential expressions in AP group.

Overall, a synergistic functioning of shrimp stress, endocrine, immune, signalling, and structural genes during pathogenic infections can be postulated which is vital for host survival and elimination of invading pathogens. Moreover, these DEGs can be jointly proposed as Survival Adaptation Molecular Patterns (SAMPs) with STAT as one of the crucial signalling components.

5.0 Conclusions

In conclusion, during WSSV and *V. parahaemolyticus/Vp_{AHPND}* infections, *MrST* gene expressions were significantly down-regulated (during either early or later post-infection time points) whereas *PmST* gene expressions were only significantly up-regulated. In addition, the sequence and structural comparison of *MrST* and *PmST* provided significant insight into the important similarities or differences between the compared shrimp STAT sequences. These differences were inferred to be one of the deciding factors resulting in the differential gene expression patterns observed. STAT gene plays vital diverse roles in JAK-STAT signalling pathway especially during pathogenic infections. Hence, the systematic comparison of selected omics data was done to identify the important DEGs (stress, endocrine, immune, signalling, and structural) in *M. rosenbergii* and *P. monodon* when exposed to WSSV and *V. parahaemolyticus/Vp_{AHPND}* infections focusing on those involved in STAT functioning or potentially associated with JAK-STAT signalling. The functional grouping of these DEGs validated the diverse signalling roles of STAT.

Overall, the findings of this study will be able to provide valuable insight for future research towards better understanding of the shrimp immune response especially STAT gene functioning. This study also possesses novelty in the emphasis of the stress and endocrine DEGs because these DEGs are easily neglected normally with more research focus given to immune DEGs. However, these DEGs are important as well because stress DEGs function as alert and trigger factors whereas endocrine DEGs function as regulatory and survival factors. The qPCR primers designed, sequence and structural divergence identified, and important DEGs obtained can be applied for shrimp health or immune response activation diagnostic purpose. STAT gene can also be proposed as a suitable candidate for the study of immune response enhancement or regulation due to its diverse signalling importance in shrimp immunity and survival.

Supporting information

S1 Fig. Relative gene expression fold change of *MrST* in response to WSSV infection. *All relative gene expression fold changes were statistically significant ($P < 0.05$). *a, b, and c represent different subsets obtained in Post Hoc Duncan Test. *The error bars indicated standard deviations of the data. [*MrST* (WSSV) Fold changes: 0 hpi: -1.113; 3 hpi: -2.332; 6 hpi: -4.699; 12 hpi: -2.038; 24 hpi: 2.287; 48 hpi: 2.017]. (DOCX)

S2 Fig. Relative gene expression fold change of *MrST* in response to *V. parahaemolyticus* infection. *All relative gene expression fold changes were statistically significant ($P < 0.05$). *a, b, c, and d represent different subsets obtained in Post Hoc Duncan Test. *The error bars indicated standard deviations of the data. [*MrST* (*V. parahaemolyticus*) Fold changes: 0 hpi: 1.238; 3 hpi: 2.272; 6 hpi: -1.766; 12 hpi: -3.262; 24 hpi: -5.429; 48 hpi: -1.125]. (DOCX)

S3 Fig. Relative gene expression fold change of *PmST* in response to WSSV infection. *All relative gene expression fold changes were statistically significant ($P < 0.05$). *a, b, and c represent different subsets obtained in Post Hoc Duncan Test. *The error bars indicated standard deviations of the data. [*PmST* (WSSV) Fold changes: 0 hpi: 1.650; 3 hpi: 1.500; 6 hpi: 1.729; 12 hpi: 7.082; 24 hpi: 10.691; 48 hpi: 2.510]. (DOCX)

S4 Fig. Relative gene expression fold change of *PmST* in response to *Vp_{AHPND}* infection. *All relative gene expression fold changes were statistically significant ($P < 0.05$). *a, b, and c represent different subsets obtained in Post Hoc Duncan Test. *The error bars indicated standard deviations of the data. [*PmST* (*Vp_{AHPND}*) Fold changes: 0 hpi: 1.622; 3 hpi: 3.059; 6 hpi: 2.500; 12 hpi: 2.298; 24 hpi: 3.139; 48 hpi: 1.273]. (DOCX)

S5 Fig. Sequence comparison of *MrST*, *LvST*, *PmST* (cross-bred disease tolerant strain [labelled as *PmST*(New)], and *PmST* (Accession number: AY327491.1) STAT nucleotide sequences using Clustal Omega software. * represents common conserved sites between all sequences. | represents the start and stop codons of the ORF regions. — represents important long conserved overlaps between all sequences. ↗ represents important divergent sites between *PmST* (cross-bred disease tolerant strain) and *PmST* (Accession number: AY327491.1). ↗ represents important divergent sites between *MrST* and other STAT sequences. □ represents important nucleotide addition or deletion between *MrST* and other STAT sequences. (DOCX)

S6 Fig. Phylogenetic comparison of *M. rosenbergii* STAT (*MrST*) and *P. monodon* STAT (*PmST*) (disease tolerant strain and AY327491.1) sequences with 13 homologous sequences retrieved from NCBI database using MEGA 7 software through Maximum Likelihood method with bootstrap value of 1000. A) Phylogenetic tree generated from *M. rosenbergii* STAT (*MrST*), *P. monodon* STAT (*PmST*) (disease tolerant strain and AY327491.1), and other homologous STAT nucleotide sequences (Tamura-Nei model). B) Phylogenetic tree generated from *M. rosenbergii* STAT (*MrST*), *P. monodon* STAT (*PmST*) (cross-bred disease tolerant strain and AY327491.1), and other homologous STAT amino acid sequences (Jones-Taylor-Thornton (JTT) model). **PmST* (disease tolerant strain) nucleotide and amino acid sequences were labelled as “New”. (DOCX)

S7 Fig. Nucleotide and translated amino acid sequences of *M. rosenbergii* STAT (*MrST*). A) Nucleotide sequence of *M. rosenbergii* STAT (*MrST*) obtained (full coding sequence). A total of 2906 base pair (bp) were observed for *MrST*, with an ORF of 2436 bp (ORF labelled in blue). B) *MrST* amino acid sequence numbered from N-terminus aligned with respective ORF nucleotide sequence. The protein consists of 811 amino acids (amino acid labelled in blue). (DOCX)

S8 Fig. Nucleotide and translated amino acid sequences of *P. monodon* STAT (PmST). A) Nucleotide sequence of *Penaeus monodon* STAT (*PmST*) obtained (full coding sequence). A total of 2491 base pair (bp) were observed for *PmST*, with an ORF of 2340 bp (ORF labelled in blue). B) PmST amino acid sequence numbered from N-terminus aligned with respective ORF nucleotide sequence. The protein consists of 779 amino acids (amino acid labelled in blue). (DOCX)

S9 Fig. NCBI Conserved Domain Search of *M. rosenbergii* STAT (MrST) and *P. monodon* STAT (PmST). A) NCBI Conserved Domain Search of MrST protein sequence demonstrating four functional domains, namely STAT_int (17 aa-141 aa), STAT5_CCD (159 aa-352 aa), STAT_bind (354 aa-603 aa), and SH2_STAT (594 aa-710 aa). B) NCBI Conserved Domain Search of PmST protein sequence demonstrating four functional domains, namely STAT_int (7 aa-133 aa), STAT5_CCD (150 aa-343 aa), STAT_bind (345 aa-592 aa), and SH2_STAT (583 aa-699 aa). (DOCX)

S10 Fig. Secondary Structure Prediction of *M. rosenbergii* STAT (MrST) and *P. monodon* STAT (PmST) (Cross-bred Disease Tolerant Strain) Protein Sequences using PSIPRED. A) Predicted secondary structure of *M. rosenbergii* STAT (MrST) protein sequence. B) Predicted secondary structure of *P. monodon* STAT (PmST) protein sequence. (DOCX)

S11 Fig. Protein Domains, Families, and Functional Sites Prediction of *M. rosenbergii* STAT (MrST) and *P. monodon* STAT (PmST) Protein Sequences using PROSITE. A) Predicted domains, families, and functional sites of *M. rosenbergii* STAT (MrST) protein sequence. B) Predicted domains, families, and functional sites of *P. monodon* STAT (PmST) protein sequence. (DOCX)

S12 Fig. 3D Protein Structure Prediction of *M. rosenbergii* STAT (MrST) and *P. monodon* STAT (PmST) Protein Sequences using SWISS-MODEL. A) Predicted 3D protein structure of *M. rosenbergii* STAT (MrST) protein sequence. B) Predicted 3D protein structure of *P. monodon* STAT (PmST) protein sequence. (DOCX)

S1 Table. The list of gene, primer pair, and probe sequences used in the qPCR experiments. (DOCX)

S2 Table. The list of gene and primer pair sequences used in the PCR experiments. (DOCX)

S3 Table. Statistical significance validation of *MrST* relative gene expression in response to WSSV infection using (A) One-Way ANOVA and (B) Post Hoc Duncan Test. (DOCX)

S4 Table. Statistical significance validation of *MrST* relative gene expression in response to *V. parahaemolyticus* infection using (A) One-Way ANOVA and (B) Post Hoc Duncan Test. (DOCX)

S5 Table. Statistical significance validation of *PmST* relative gene expression in response to WSSV infection using (A) One-Way ANOVA and (B) Post Hoc Duncan Test.

(DOCX)

S6 Table. Statistical significance validation of *PmST* relative gene expression in response to *Vp*_{AHPND} infection using (A) One-Way ANOVA and (B) Post Hoc Duncan Test.

(DOCX)

S7 Table. Detailed comparison of important transcriptomic DEGs identified from WSSV and *V. parahaemolyticus*/*Vp*_{AHPND}-infected *M. rosenbergii* and *P. monodon* samples.

(DOCX)

S1 Data. Raw data of qPCR analysis.

(ZIP)

S1 Graphical Abstract.

(PDF)

Acknowledgments

The authors would like to acknowledge all the help and support received in conducting the challenge experiments, sample collections, and gene expression quantifications from AGAGEL lab members. This includes a special thanks to Ramarao Seriramalu for partial data collection of STAT gene expression quantification results. We would also like to extend gratitude to Prof Sharif who led the Technofund project in collaboration with Industry.

Author Contributions

Conceptualization: Subha Bhassu.

Data curation: Tze Chiew Christie Soo.

Formal analysis: Tze Chiew Christie Soo.

Investigation: Tze Chiew Christie Soo, Subha Bhassu.

Methodology: Tze Chiew Christie Soo, Subha Bhassu.

Project administration: Subha Bhassu.

Supervision: Subha Bhassu.

Validation: Subha Bhassu.

Visualization: Tze Chiew Christie Soo, Subha Bhassu.

Writing – original draft: Tze Chiew Christie Soo.

Writing – review & editing: Subha Bhassu.

References

1. Dastidar PG, Mallik A, Mandal N. Contribution of shrimp disease research to the development of the shrimp aquaculture industry: an analysis of the research and innovation structure across the countries. *Scientometrics*. 2013; 97(3): 659–674.
2. FAO. The State of World Fisheries and Aquaculture 2020: Sustainability in action. Rome: FAO; 2020.
3. Anderson JL, Valderrama D, Jory D. Shrimp production review. Global Aquaculture Alliance: Presentation Global Aquaculture Production Data and Analysis [Internet]. 2016 [cited 2021 April 9]. <https://www.aquaculturealliance.org/wp-content/uploads/2018/01/Global-Shrimp-Production-Data-Analysis-Dr.-James-Anderson-GOAL-2017.pdf>.

4. Thitamadee S, Prachumwat A, Srisala J, Jaroenlak P, Salachan PV, Sritunyalucksana K, et al. Review of current disease threats for cultivated penaeid shrimp in Asia. *Aquaculture*. 2016; 452: 69–87.
5. Ganjoor M. A short review on infectious viruses in cultural shrimps (Penaeidae family). *J Fishscicom*. 2015; 9(3): 9–33.
6. Mayo M. A summary of taxonomic changes recently approved by ICTV. *Arch Virol*. 2002; 147(8): 1655–1656. <https://doi.org/10.1007/s007050200039> PMID: 12181683
7. Walker PJ, Mohan CV. Viral disease emergence in shrimp aquaculture: origins, impact and the effectiveness of health management strategies. *Rev Aquac*. 2009; 1(2): 125–154. <https://doi.org/10.1111/j.1753-5131.2009.01007.x> PMID: 32328167
8. Zhan WB, Wang YH, Fryer JL, Yu KK, Fukuda H, Meng QX. White spot syndrome virus infection of cultured shrimp in China. *J Aquat Anim Health*. 1998; 10(4): 405–410.
9. Lee CT, Chen IT, Yang YT, Ko TP, Huang YT, Huang JY et al. The opportunistic marine pathogen *Vibrio parahaemolyticus* becomes virulent by acquiring a plasmid that expresses a deadly toxin. *Proc Natl Acad Sci USA*. 2015; 112(34): 10798–10803. <https://doi.org/10.1073/pnas.1503129112> PMID: 26261348
10. Tran L, Nunan L, Redman RM, Mohney LL, Pantoja CR, Fitzsimmons K, et al. Determination of the infectious nature of the agent of acute hepatopancreatic necrosis syndrome affecting penaeid shrimp. *Dis Aquat Org*. 2013; 105(1): 45–55. <https://doi.org/10.3354/dao02621> PMID: 23836769
11. FAO. Report of the FAO/MARD technical workshop on early mortality syndrome (EMS) or acute hepatopancreatic necrosis syndrome (AHPNS) of cultured shrimp (UNDER TCP/VIE/3304). Rome: FAO; 2013.
12. Nunan L, Lightner D, Pantoja C, Gomez-Jimenez S. Detection of acute hepatopancreatic necrosis disease (AHPND) in Mexico. *Dis Aquat Org*. 2014; 111(1): 81–86.
13. Hong X, Lu L, Xu D. Progress in research on acute hepatopancreatic necrosis disease (AHPND). *Aquac Int*. 2016; 24(2): 577–593.
14. Zorriehzakra MJ, Banaederakhshan R. Early mortality syndrome (EMS) as new emerging threat in shrimp industry. *Adv Anim Vet Sci*. 2015; 3(2S): 64–72.
15. Khuntia CP, Das BK, Samantaray BR, Samal SK, Mishra BK. Characterization and pathogenicity studies of *Vibrio parahaemolyticus* isolated from diseased freshwater prawn, *Macrobrachium rosenbergii* (de Man). *Aquac Res*. 2008; 39(3): 301–310.
16. Schofield PJ, Noble BL, Caro LFA, Mai HN, Padilla TJ, Millabas J, et al. Pathogenicity of Acute Hepatopancreatic Necrosis Disease (AHPND) on the freshwater prawn, *Macrobrachium rosenbergii*, and Pacific White Shrimp, *Penaeus vannamei*, at various salinities. *Aquac Res*. 2021; 52(4): 1480–1489.
17. Moss SM, Moss DR, Arce SM, Lightner DV, Lotz JM. The role of selective breeding and biosecurity in the prevention of disease in penaeid shrimp aquaculture. *J Invertebr Pathol*. 2012; 110(2): 247–250. <https://doi.org/10.1016/j.jip.2012.01.013> PMID: 22434005
18. Uddin SA, Kader MA. The use of antibiotics in shrimp hatcheries in Bangladesh. *J Fish Aquat Sci*. 2006; 1(1): 64–67.
19. Farzanfar A. The use of probiotics in shrimp aquaculture. *FEMS Immunol Med Microbiol*. 2006; 48(2): 149–158. <https://doi.org/10.1111/j.1574-695X.2006.00116.x> PMID: 17064272
20. Liongue C, O'Sullivan LA, Trengove MC, Ward AC. Evolution of JAK-STAT pathway components: mechanisms and role in immune system development. *PLoS One*. 2012; 7(3): e32777. <https://doi.org/10.1371/journal.pone.0032777> PMID: 22412924
21. O'Shea JJ, Holland SM, Staudt LM. JAKs and STATs in immunity, immunodeficiency, and cancer. *N Engl J Med*. 2013; 368(2): 161–170. <https://doi.org/10.1056/NEJMra1202117> PMID: 23301733
22. Nicolas CS, Amici M, Bortolotto ZA, Doherty A, Csaba Z, Fafouri A, et al. The role of JAK-STAT signaling within the CNS. *JAKSTAT*. 2013; 2(1): e22925. <https://doi.org/10.4161/jkst.22925> PMID: 24058789
23. Gorissen M, Vrieze ED, Flik G, Huising MO. STAT genes display differential evolutionary rates that correlate with their roles in the endocrine and immune system. *J Endocrinol*. 2011; 209: 175–184. <https://doi.org/10.1530/JOE-11-0033> PMID: 21330334
24. La Fortezza M, Schenk M, Cosolo A, Kolybaba A, Grass I, Classen AK. JAK/STAT signalling mediates cell survival in response to tissue stress. *Development*. 2016; 143(16): 2907–2919. <https://doi.org/10.1242/dev.132340> PMID: 27385008
25. Dodington DW, Desai HR, Woo M. JAK/STAT—emerging players in metabolism. *Trends Endocrinol Metab*. 2018; 29(1): 55–65. <https://doi.org/10.1016/j.tem.2017.11.001> PMID: 29191719
26. Chen W, Daines MO, Hershey GKK. Turning off signal transducer and activator of transcription (STAT): the negative regulation of STAT signaling. *J Allergy Clin Immunol*. 2004; 114(3): 476–489. <https://doi.org/10.1016/j.jaci.2004.06.042> PMID: 15356544

27. Cheng CH, Chen GD, Yeh MS, Chu CY, Hsu YL, Hwang PP, et al. Expression and characterization of the JAK kinase and STAT protein from brine shrimp, *Artemia franciscana*. *Fish Shellfish Immunol*. 2010; 28(5–6): 774–782. <https://doi.org/10.1016/j.fsi.2010.01.022> PMID: 20156563
28. Niu GJ, Xu JD, Yuan WJ, Sun JJ, Yang MC, He ZH, et al. Protein inhibitor of activated STAT (PIAS) negatively regulates the JAK/STAT pathway by inhibiting STAT phosphorylation and translocation. *Front Immunol*. 2018; 9: 2392. <https://doi.org/10.3389/fimmu.2018.02392> PMID: 30416501
29. Okugawa S, Mekata T, Inada M, Kihara K, Shiki A, Kannabiran K, et al. The SOCS and STAT from JAK/STAT signaling pathway of kuruma shrimp *Marsupenaeus japonicus*: molecular cloning, characterization and expression analysis. *Mol Cell Probes*. 2013; 27(1): 6–14. <https://doi.org/10.1016/j.mcp.2012.08.003> PMID: 22921512
30. Sun C, Shao HL, Zhang XW, Zhao XF, Wang JX. Molecular cloning and expression analysis of signal transducer and activator of transcription (STAT) from the Chinese white shrimp *Fenneropenaeus chinensis*. *Mol. Biol. Rep*. 2011; 38(8): 5313–5319. <https://doi.org/10.1007/s11033-011-0681-x> PMID: 21246285
31. Ren Q, Huang Y, He Y, Wang W, Zhang X. A white spot syndrome virus microRNA promotes the virus infection by targeting the host STAT. *Sci. Rep*. 2015; 5(1): 1–12.
32. Wen R, Li F, Li S, Xiang J. Function of shrimp STAT during WSSV infection. *Fish Shellfish Immunol*. 2014; 38(2): 354–360. <https://doi.org/10.1016/j.fsi.2014.04.002> PMID: 24727196
33. Chen Q, Zhang Z, Tang H, Zhou L, Ao S, Zhou Y, et al. *Aeromonas hydrophila* associated with red spot disease in *Macrobrachium nipponense* and host immune-related gene expression profiles. *J. Invertebr. Pathol*. 2021; 182: 107584. <https://doi.org/10.1016/j.jip.2021.107584> PMID: 33811849
34. Li X, Yang H, Gao X, Zhang H, Chen N, Miao Z, et al. The pathogenicity characterization of non-O1 *Vibrio cholerae* and its activation on immune system in freshwater shrimp *Macrobrachium nipponense*. *Fish Shellfish Immunol*. 2019; 87: 507–514. <https://doi.org/10.1016/j.fsi.2019.01.050> PMID: 30711493
35. Yao D, Ruan L, Lu H, Shi H, Xu X. Shrimp STAT was hijacked by white spot syndrome virus immediate-early protein IE1 involved in modulation of viral genes. *Fish Shellfish Immunol*. 2016; 59: 268–275. <https://doi.org/10.1016/j.fsi.2016.10.051> PMID: 27815197
36. Giulietti A, Overbergh L, Valckx D, Decallonne B, Bouillon R, Mathieu C. An overview of real-time quantitative PCR: applications to quantify cytokine gene expression. *Methods*. 2001; 25(4): 386–401. <https://doi.org/10.1006/meth.2001.1261> PMID: 11846608
37. Raghavachari N, Garcia-Reyero N. Overview of gene expression analysis: transcriptomics. In *Gene Expression Analysis*. New York: Humana Press; 2018. pp. 1–6.
38. Derveaux S, Vandesompele J, Hellems J. How to do successful gene expression analysis using real-time PCR. *Methods*. 2010; 50(4): 227–230. <https://doi.org/10.1016/j.ymeth.2009.11.001> PMID: 19969088
39. Morozova O, Hirst M, Marra MA. Applications of new sequencing technologies for transcriptome analysis. *Annu Rev Genomics Hum Genet*. 2009; 10: 135–151. <https://doi.org/10.1146/annurev-genom-082908-145957> PMID: 19715439
40. Kimura T, Yamano K, Nakano H, Momoyama K, Hiraoka M, Inouye K. Detection of penaeid rod-shaped DNA virus (PRDV) by PCR. *Fish Pathol*. 1996; 31(2): 93–98.
41. Supamattaya K, Hoffmann RW, Boonyaratpalin S, Kanchanaphum P. Experimental transmission of white spot syndrome virus (WSSV) from black tiger shrimp *Penaeus monodon* to the sand crab *Portunus pelagicus*, mud crab *Scylla serrata* and krill *Acetes* sp. *Dis Aquat Organ*. 1998; 32(2): 79–85.
42. Mendoza-Cano F, Sánchez-Paz A. Development and validation of a quantitative real-time polymerase chain assay for universal detection of the White Spot Syndrome Virus in marine crustaceans. *Virology*. 2013; 10(1): 1–11. <https://doi.org/10.1186/1743-422X-10-186> PMID: 23758658
43. Sirikharin R, Taengchaiyaphum S, Sanguanrut P, Chi TD, Mavichak R, Proespraiwong P, et al. Characterization and PCR detection of binary, Pir-like toxins from *Vibrio parahaemolyticus* isolates that cause acute hepatopancreatic necrosis disease (AHPND) in shrimp. *PLoS One*. 2015; 10(5): e0126987. <https://doi.org/10.1371/journal.pone.0126987> PMID: 26017673
44. Soo TCC, Devadas S, Din MSM, Bhassu S. Differential transcriptome analysis of the disease tolerant Madagascar–Malaysia crossbred black tiger shrimp, *Penaeus monodon* hepatopancreas in response to acute hepatopancreatic necrosis disease (AHPND) infection: inference on immune gene response and interaction. *Gut Pathog*. 2019; 11(1): 1–13. <https://doi.org/10.1186/s13099-019-0319-4> PMID: 31372182
45. Rao R, Zhu YB, Alinejad T, Tiruvayipati S, Thong KL, Wang J, et al. RNA-seq analysis of *Macrobrachium rosenbergii* hepatopancreas in response to *Vibrio parahaemolyticus* infection. *Gut Pathog*. 2015; 7(1): 1–16.
46. Rao R, Bhassu S, Bing RZY, Alinejad T, Hassan SS, Wang J. A transcriptome study on *Macrobrachium rosenbergii* hepatopancreas experimentally challenged with white spot syndrome virus

- (WSSV). *J Invertebr Pathol.* 2016; 136: 10–22. <https://doi.org/10.1016/j.jip.2016.01.002> PMID: 26880158
47. Ghani FM, Bhassu S. A new insight to biomarkers related to resistance in survived-white spot syndrome virus challenged giant tiger shrimp, *Penaeus monodon*. *PeerJ.* 2019; 7: e8107. <https://doi.org/10.7717/peerj.8107> PMID: 31875142
 48. Devadas S, Bhassu S, Soo TCC, Iqbal SNM, Yusoff FM, Shariff M. Draft genome sequence of a *Vibrio parahaemolyticus* strain, KS17. S5-1, with multiple antibiotic resistance genes, which causes acute hepatopancreatic necrosis disease in *Penaeus monodon* in the West Coast of Peninsular Malaysia. *Microbiol Resour Announc.* 2018; 7(2): 1–2. <https://doi.org/10.1128/MRA.00829-18> PMID: 30533806
 49. Dhar AK, Bowers RM, Licon KS, Veazey G, Read B. Validation of reference genes for quantitative measurement of immune gene expression in shrimp. *Mol Immunol.* 2009; 46(8–9): 1688–1695. <https://doi.org/10.1016/j.molimm.2009.02.020> PMID: 19297025
 50. Ramarao S. Transcriptome analysis of immune responses in *Macrobrachium rosenbergii* against white spot syndrome virus and *Vibrio parahaemolyticus* [D. Phil. Thesis]. Kuala Lumpur: University of Malaya; 2017.
 51. Livak KJ, Schmittgen TD. Analysis of relative gene expression data using real-time quantitative PCR and the $2^{-\Delta\Delta CT}$ method. *Methods.* 2001; 25(4): 402–408. <https://doi.org/10.1006/meth.2001.1262> PMID: 11846609
 52. Kumar S, Stecher G, Tamura K. MEGA7: molecular evolutionary genetics analysis version 7.0 for bigger datasets. *Mol Biol Evol.* 2016; 33(7): 1870–1874. <https://doi.org/10.1093/molbev/msw054> PMID: 27004904
 53. Altschul SF, Gish W, Miller W, Myers EW, Lipman DJ. Basic local alignment search tool. *J Mol Biol.* 1990; 215(3): 403–410. [https://doi.org/10.1016/S0022-2836\(05\)80360-2](https://doi.org/10.1016/S0022-2836(05)80360-2) PMID: 2231712
 54. Marchler-Bauer A, Derbyshire MK, Gonzales NR, Lu S, Chitsaz F, Geer LY, et al. CDD: NCBI's conserved domain database. *Nucleic Acids Res.* 2015; 43(D1): D222–D226. <https://doi.org/10.1093/nar/gku1221> PMID: 25414356
 55. Omasits U, Ahrens CH, Müller S, Wollscheid B. Protter: interactive protein feature visualization and integration with experimental proteomic data. *Bioinformatics.* 2014; 30(6): 884–886. <https://doi.org/10.1093/bioinformatics/btt607> PMID: 24162465
 56. Blum T, Briesemeister S, Kohlbacher O. MultiLoc2: integrating phylogeny and Gene Ontology terms improves subcellular protein localization prediction. *BMC Bioinformatics.* 2009; 10(1): 1–11. <https://doi.org/10.1186/1471-2105-10-274> PMID: 19723330
 57. Lorenz R, Bernhart SH, Zu Siederdisen CH, Tafer H, Flamm C, Stadler PF, et al. ViennaRNA Package 2.0. *Algorithms Mol Biol.* 2011; 6(1): 1–14.
 58. Buchan DW, Jones DT. The PSIPRED protein analysis workbench: 20 years on. *Nucleic Acids Res.* 2019; 47(W1): W402–W407. <https://doi.org/10.1093/nar/gkz297> PMID: 31251384
 59. Hulo N, Bairoch A, Bulliard V, Cerutti L, De Castro E, Langendijk-Genevaux PS, et al. The PROSITE database. *Nucleic Acids Res.* 2006; 34(suppl_1): D227–D230. <https://doi.org/10.1093/nar/gkj063> PMID: 16381852
 60. Waterhouse A, Bertoni M, Bienert S, Studer G, Tauriello G, Gumienny R, et al. SWISS-MODEL: homology modelling of protein structures and complexes. *Nucleic Acids Res.* 2018; 46(W1): W296–W303. <https://doi.org/10.1093/nar/gky427> PMID: 29788355
 61. Loveday EK, Diederich S, Pasick J, Jean F. Human microRNA-24 modulates highly pathogenic avian-origin H5N1 influenza A virus infection in A549 cells by targeting secretory pathway furin. *J. Gen. Virol.* 2015; 96(1): 30–39. <https://doi.org/10.1099/vir.0.068585-0> PMID: 25234642
 62. Syed Musthaq S, Kwang J. Oral vaccination of baculovirus-expressed VP28 displays enhanced protection against white spot syndrome virus in *Penaeus monodon*. *PLoS One.* 2011; 6(11): e26428. <https://doi.org/10.1371/journal.pone.0026428> PMID: 22069450
 63. Thomas A, Sudheer NS, Kiron V, Singh ISB, Narayanan RB. Expression profile of key immune-related genes in *Penaeus monodon* juveniles after oral administration of recombinant envelope protein VP28 of white spot syndrome virus. *Microb Pathog.* 2016; 96: 72–79. <https://doi.org/10.1016/j.micpath.2016.05.002> PMID: 27154537
 64. Deng H, Zhang W, Li J, Li J, Hu L, Yan W, et al. A signal transducers and activators of transcription (STAT) gene from *Scylla paramamosain* is involved in resistance against mud crab reovirus. *Fish Shellfish Immunol.* 2019; 94: 580–591. <https://doi.org/10.1016/j.fsi.2019.09.045> PMID: 31539571
 65. Sun JJ, Lan JF, Zhao XF, Vasta GR, Wang JX. Binding of a C-type lectin's coiled-coil domain to the Domeless receptor directly activates the JAK/STAT pathway in the shrimp immune response to bacterial infection. *PLoS Pathog.* 2017; 13(9): e1006626. <https://doi.org/10.1371/journal.ppat.1006626> PMID: 28931061

66. Yamauchi MM, Miya MU, Machida RJ, Nishida M. PCR-based approach for sequencing mitochondrial genomes of decapod crustaceans, with a practical example from kuruma prawn (*Marsupenaeus japonicus*). *Mar. Biotechnol.* 2004; 6(5): 419–429.
67. Delisle I, Strobeck C. Conserved primers for rapid sequencing of the complete mitochondrial genome from carnivores, applied to three species of bears. *Mol. Biol. Evol.* 2002; 19(3): 357–361. <https://doi.org/10.1093/oxfordjournals.molbev.a004090> PMID: 11861896
68. Ren Q, Du ZQ, Li M, Zhang CY, Chen KP. Cloning and expression analysis of an anti-lipopolysaccharide factor from giant freshwater prawn, *Macrobrachium rosenbergii*. *Mol. Biol. Rep.* 2012; 39(7): 7673–7680. <https://doi.org/10.1007/s11033-012-1602-3> PMID: 22350161
69. DeBoever C, Li H, Jakubosky D, Benaglio P, Reyna J, Olson KM, et al. Large-scale profiling reveals the influence of genetic variation on gene expression in human induced pluripotent stem cells. *Cell Stem Cell.* 2017; 20(4): 533–546. <https://doi.org/10.1016/j.stem.2017.03.009> PMID: 28388430
70. Deelen P, Zhernakova DV, de Haan M, van der Sijde M, Bonder MJ, Karjalainen J, et al. Calling genotypes from public RNA-sequencing data enables identification of genetic variants that affect gene-expression levels. *Genome Med.* 2015; 7(1): 1–13.
71. Burgess WH, Shaheen AM, Ravera M, Jaye M, Donohue PJ, Winkles JA. Possible dissociation of the heparin-binding and mitogenic activities of heparin-binding (acidic fibroblast) growth factor-1 from its receptor-binding activities by site-directed mutagenesis of a single lysine residue. *J Cell Biol.* 1990; 111(5): 2129–2138. <https://doi.org/10.1083/jcb.111.5.2129> PMID: 1699952
72. Cho W, Taylor LP, Mansour A, Akil H. Hydrophobic residues of the D2 dopamine receptor are important for binding and signal transduction. *J Neurochem.* 1995; 65(5): 2105–2115. <https://doi.org/10.1046/j.1471-4159.1995.65052105.x> PMID: 7595496
73. Loo TW, Clarke DM. Functional consequences of phenylalanine mutations in the predicted transmembrane domain of P-glycoprotein. *J Biol Chem.* 1993; 268(27): 19965–19972. PMID: 8104183
74. Holloway AK, Lawniczak MK, Mezey JG, Begun DJ, Jones CD. Adaptive gene expression divergence inferred from population genomics. *PLoS Genet.* 2007; 3(10): e187. <https://doi.org/10.1371/journal.pgen.0030187> PMID: 17967066
75. Yamauchi MM, Miya MU, Nishida M. Complete mitochondrial DNA sequence of the swimming crab, *Portunus trituberculatus* (Crustacea: Decapoda: Brachyura). *Gene.* 2003; 311: 129–135. [https://doi.org/10.1016/s0378-1119\(03\)00582-1](https://doi.org/10.1016/s0378-1119(03)00582-1) PMID: 12853147
76. Kiraga J, Mackiewicz P, Mackiewicz D, Kowalczyk M, Biecek P, Polak N, et al. The relationships between the isoelectric point and: length of proteins, taxonomy and ecology of organisms. *BMC Genomics.* 2007; 8(1): 1–16. <https://doi.org/10.1186/1471-2164-8-163> PMID: 17565672
77. Heim MH, Kerr IM, Stark GR, Darnell JE. Contribution of STAT SH2 groups to specific interferon signaling by the Jak-STAT pathway. *Science.* 1995; 267(5202): 1347–1349. <https://doi.org/10.1126/science.7871432> PMID: 7871432
78. Sarathi M, Basha AN, Ravi M, Venkatesan C, Kumar BS, Hameed AS. Clearance of white spot syndrome virus (WSSV) and immunological changes in experimentally WSSV-injected *Macrobrachium rosenbergii*. *Fish Shellfish Immunol.* 2008; 25(3): 222–230. <https://doi.org/10.1016/j.fsi.2008.04.011> PMID: 18603447
79. Hu WY, Yao CL. Molecular and immune response characterizations of a novel AIF and cytochrome c in *Litopenaeus vannamei* defending against WSSV infection. *Fish Shellfish Immunol.* 2016; 56: 84–95. <https://doi.org/10.1016/j.fsi.2016.06.050> PMID: 27368536
80. Junprung W, Supungul P, Tassanakajon A. HSP70 and HSP90 are involved in shrimp *Penaeus vannamei* tolerance to AHPND-causing strain of *Vibrio parahaemolyticus* after non-lethal heat shock. *Fish Shellfish Immunol.* 2017; 60: 237–246. <https://doi.org/10.1016/j.fsi.2016.11.049> PMID: 27888131
81. Rauschenbach IY, Karpova EK, Adonyeva NV, Andreenkova OV, Faddeeva NV, Burdina EV, et al. Disruption of insulin signalling affects the neuroendocrine stress reaction in *Drosophila* females. *J Exp Biol.* 2014; 217(20): 3733–3741. <https://doi.org/10.1242/jeb.106815> PMID: 25214494
82. Yamaguchi A, Hori O, Stern DM, Hartmann E, Ogawa S, Tohyama M. Stress-associated endoplasmic reticulum protein 1 (SERP1)/Ribosome-associated membrane protein 4 (RAMP4) stabilizes membrane proteins during stress and facilitates subsequent glycosylation. *J Cell Biol.* 1999; 147(6): 1195–1204. <https://doi.org/10.1083/jcb.147.6.1195> PMID: 10601334
83. Li E, Wang X, Chen K, Xu C, Qin JG, Chen L. Physiological change and nutritional requirement of Pacific white shrimp *Litopenaeus vannamei* at low salinity. *Rev Aquac.* 2017; 9(1): 57–75.
84. Pascual C, Zenteno E, Cuzon G, Sánchez A, Gaxiola G, Taboada G, et al. *Litopenaeus vannamei* juveniles energetic balance and immunological response to dietary protein. *Aquaculture.* 2004; 236(1–4): 431–450.

85. Qi C, Wang L, Liu M, Jiang K, Wang M, Zhao W, et al. Transcriptomic and morphological analyses of *Litopenaeus vannamei* intestinal barrier in response to *Vibrio parahaemolyticus* infection reveals immune response signatures and structural disruption. *Fish Shellfish Immunol.* 2017; 70: 437–450. <https://doi.org/10.1016/j.fsi.2017.09.004> PMID: 28889014
86. Adams DJ, Barakeh J, Laskey R, Van Breemen C. Ion channels and regulation of intracellular calcium in vascular endothelial cells. *FASEB J.* 1989; 3(12): 2389–2400. <https://doi.org/10.1096/fasebj.3.12.2477294> PMID: 2477294
87. Ju H, Venema VJ, Liang H, Harris MB, Zou R, Venema RC. Bradykinin activates the Janus-activated kinase/signal transducers and activators of transcription (JAK/STAT) pathway in vascular endothelial cells: localization of JAK/STAT signalling proteins in plasmalemmal caveolae. *Biochem J.* 2000; 351(1): 257–264. <https://doi.org/10.1042/0264-6021:3510257> PMID: 10998369
88. Ryan CP, Brownlie JC, Whyard S. Hsp90 and physiological stress are linked to autonomous transposon mobility and heritable genetic change in nematodes. *Genome Biol Evol.* 2016; 8(12): 3794–3805. <https://doi.org/10.1093/gbe/evw284> PMID: 28082599
89. Sato N, Yamamoto T, Sekine Y, Yumioka T, Junicho A, Fuse H, et al. Involvement of heat-shock protein 90 in the interleukin-6-mediated signaling pathway through STAT3. *Biochem Biophys Res Commun.* 2003; 300(4): 847–852. [https://doi.org/10.1016/s0006-291x\(02\)02941-8](https://doi.org/10.1016/s0006-291x(02)02941-8) PMID: 12559950
90. Zhang H, Burrows F. Targeting multiple signal transduction pathways through inhibition of Hsp90. *J Mol Med.* 2004; 82(8): 488–499. <https://doi.org/10.1007/s00109-004-0549-9> PMID: 15168026
91. Chin YE, Kitagawa M, Kuida K, Flavell RA, Fu XY. Activation of the STAT signaling pathway can cause expression of caspase 1 and apoptosis. *Mol Cell Biol.* 1997; 17(9): 5328. <https://doi.org/10.1128/MCB.17.9.5328> PMID: 9271410
92. Hao XR, Cao DL, Hu YW, Li XX, Liu XH, Xiao J, et al. IFN- γ down-regulates ABCA1 expression by inhibiting LXR α in a JAK/STAT signaling pathway-dependent manner. *Atherosclerosis.* 2009; 203(2): 417–428. <https://doi.org/10.1016/j.atherosclerosis.2008.07.029> PMID: 18789440
93. Wang XW, Vasta GR, Wang JX. The functional relevance of shrimp C-type lectins in host-pathogen interactions. *Dev Comp Immunol.* 2020; 109: 103708. <https://doi.org/10.1016/j.dci.2020.103708> PMID: 32305304
94. Jounai N, Kobiyama K, Takeshita F, Ishii KJ. Recognition of damage-associated molecular patterns related to nucleic acids during inflammation and vaccination. *Front Cell Infect Microbiol.* 2013; 2: 168. <https://doi.org/10.3389/fcimb.2012.00168> PMID: 23316484
95. Liu H, Yao YM, Yu Y, Dong N, Yin HN, Sheng ZY. Role of Janus kinase/signal transducer and activator of transcription pathway in regulation of expression and inflammation-promoting activity of high mobility group box protein 1 in rat peritoneal macrophages. *Shock.* 2007; 27(1): 55–60. <https://doi.org/10.1097/01.shk.0000233197.40989.31> PMID: 17172981
96. Yang L, Luo M, He J, Zuo H, Weng S, He J, et al. A JAK-STAT pathway target gene encoding a single WAP domain (SWD)-containing protein from *Litopenaeus vannamei*. *Fish Shellfish Immunol.* 2019; 89: 555–563. <https://doi.org/10.1016/j.fsi.2019.04.046> PMID: 30999041
97. Ighodaro OM, Akinloye OA. First line defence antioxidants-superoxide dismutase (SOD), catalase (CAT) and glutathione peroxidase (GPX): Their fundamental role in the entire antioxidant defence grid. *Alexandria J Med.* 2018; 54(4): 287–293.
98. Jung JE, Kim GS, Narasimhan P, Song YS, Chan PH. Regulation of Mn-superoxide dismutase activity and neuroprotection by STAT3 in mice after cerebral ischemia. *J. Neurosci.* 2009; 29(21): 7003–7014. <https://doi.org/10.1523/JNEUROSCI.1110-09.2009> PMID: 19474327
99. Prater MR, Lauderilch CL, Holladay SD. Does immune stimulation or antioxidant therapy reduce MNU-induced placental damage via activation of Jak-STAT and NF κ B signaling pathways?. *Placenta.* 2007; 28(5–6): 566–570. <https://doi.org/10.1016/j.placenta.2006.05.002> PMID: 16822543
100. Liu D, Sheng C, Gao S, Yao C, Li J, Jiang W, et al. SOCS3 drives proteasomal degradation of TBK1 and negatively regulates antiviral innate immunity. *Mol Cell Biol.* 2015; 35(14): 2400. <https://doi.org/10.1128/MCB.00090-15> PMID: 25939384
101. Cai B, Li J, Wang J, Luo X, Ai J, Liu Y, et al. microRNA-124 regulates cardiomyocyte differentiation of bone marrow-derived mesenchymal stem cells via targeting STAT3 signaling. *Stem Cells.* 2012; 30(8): 1746–1755. <https://doi.org/10.1002/stem.1154> PMID: 22696253
102. Liu X, Li F, Zhao S, Luo Y, Kang J, Zhao H, et al. MicroRNA-124-mediated regulation of inhibitory member of apoptosis-stimulating protein of p53 family in experimental stroke. *Stroke.* 2013; 44(7): 1973–1980. <https://doi.org/10.1161/STROKEAHA.111.000613> PMID: 23696548
103. Tian YS, Zhong D, Liu QQ, Zhao XL, Sun HX, Jin J, et al. Upregulation of miR-216a exerts neuroprotective effects against ischemic injury through negatively regulating JAK2/STAT3-involved apoptosis and inflammatory pathways. *J Neurosurg.* 2018; 130(3): 977–988. <https://doi.org/10.3171/2017.5.JNS163165> PMID: 29521586

104. Lü CX, Fan TJ, Hu GB, Cong RS. Apoptosis-inducing factor and apoptosis. *Acta Biochim Biophys Sin.* 2003; 35(10): 881–885. PMID: [14515203](https://pubmed.ncbi.nlm.nih.gov/14515203/)
105. Madan E, Prasad S, Roy P, George J, Shukla Y. Regulation of apoptosis by resveratrol through JAK/STAT and mitochondria mediated pathway in human epidermoid carcinoma A431 cells. *Biochem Biophys Res Commun.* 2008; 377(4): 1232–1237. <https://doi.org/10.1016/j.bbrc.2008.10.158> PMID: [18996091](https://pubmed.ncbi.nlm.nih.gov/18996091/)
106. Jiang L, Chen T, Xiong L, Xu JH, Gong AY, Dai B, et al. Knockdown of m6A methyltransferase METTL3 in gastric cancer cells results in suppression of cell proliferation. *Oncol Lett.* 2020; 20(3): 2191–2198. <https://doi.org/10.3892/ol.2020.11794> PMID: [32782536](https://pubmed.ncbi.nlm.nih.gov/32782536/)
107. Angleró-Rodríguez YI, MacLeod HJ, Kang S, Carlson JS, Jupatanakul N, Dimopoulos G. *Aedes aegypti* molecular responses to Zika virus: modulation of infection by the toll and jak/stat immune pathways and virus host factors. *Front Microbiol.* 2017; 8: 2050. <https://doi.org/10.3389/fmicb.2017.02050> PMID: [29109710](https://pubmed.ncbi.nlm.nih.gov/29109710/)
108. Yadav A, Kataria MA, Saini V, Yadav A. Role of leptin and adiponectin in insulin resistance. *Clin Chim Acta.* 2013; 417: 80–84. <https://doi.org/10.1016/j.cca.2012.12.007> PMID: [23266767](https://pubmed.ncbi.nlm.nih.gov/23266767/)
109. Yoshida NL, Miyashita T, Mami U, Yamada M, Reed JC, Sugita Y, et al. Analysis of gene expression patterns during glucocorticoid-induced apoptosis using oligonucleotide arrays. *Biochem Biophys Res Commun.* 2002; 293(4): 1254–1261. [https://doi.org/10.1016/S0006-291X\(02\)00361-3](https://doi.org/10.1016/S0006-291X(02)00361-3) PMID: [12054511](https://pubmed.ncbi.nlm.nih.gov/12054511/)
110. Chen WY, Wang HC, Lo CL. Modulation of bio-defense genes in WSSV-infected *Penaeus monodon*. In: Bondad-Reantaso MG, Mohan CV, Crumlish M, Subasinghe RP, editors. *Diseases in Asian Aquaculture VI*. Manila: Asian Fisheries Society; 2008. pp. 399–408.
111. Feske S, Wulff H, Skolnik EY. Ion channels in innate and adaptive immunity. *Annu Rev Immunol.* 2015; 33: 291–353. <https://doi.org/10.1146/annurev-immunol-032414-112212> PMID: [25861976](https://pubmed.ncbi.nlm.nih.gov/25861976/)
112. Qayum AA, Hayes T, Kaplan MH. JAK-STAT Signaling in Asthma and Allergic Airway Inflammation. In: Goswami R, editor. *JAK-STAT Signaling in Diseases*. Boca Raton: CRC Press; 2020.
113. Li F, Xiang J. Signaling pathways regulating innate immune responses in shrimp. *Fish Shellfish Immunol.* 2013; 34(4): 973–980. <https://doi.org/10.1016/j.fsi.2012.08.023> PMID: [22967763](https://pubmed.ncbi.nlm.nih.gov/22967763/)